



**HAL**  
open science

## **Nacre-bionic nanocomposite membrane for efficient in-plane dissipation heat harvest under high temperature**

Jiemin Wang, Dan Liu, Quanxiang Li, Cheng Chen, Zhiqiang Chen, Minoo Naebe, Pingan Song, David Portehault, Christopher J. Garvey, Dmitri Golberg, et al.

### ► To cite this version:

Jiemin Wang, Dan Liu, Quanxiang Li, Cheng Chen, Zhiqiang Chen, et al.. Nacre-bionic nanocomposite membrane for efficient in-plane dissipation heat harvest under high temperature. *Journal of Materiomics*, 2021, 7, pp.219. 10.1016/j.jmat.2020.08.006 . hal-02993707

**HAL Id: hal-02993707**

**<https://hal.sorbonne-universite.fr/hal-02993707>**

Submitted on 6 Nov 2020

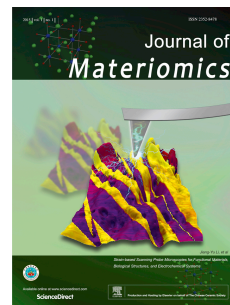
**HAL** is a multi-disciplinary open access archive for the deposit and dissemination of scientific research documents, whether they are published or not. The documents may come from teaching and research institutions in France or abroad, or from public or private research centers.

L'archive ouverte pluridisciplinaire **HAL**, est destinée au dépôt et à la diffusion de documents scientifiques de niveau recherche, publiés ou non, émanant des établissements d'enseignement et de recherche français ou étrangers, des laboratoires publics ou privés.

# Journal Pre-proof

Nacre-bionic nanocomposite membrane for efficient in-plane dissipation heat harvest under high temperature

Jiemin Wang, Dan Liu, Quanxiang Li, Cheng Chen, Zhiqiang Chen, Mino Naebe, Pingan Song, David Portehault, Christopher J. Garvey, Dmitri Golberg, Weiwei Lei



PII: S2352-8478(20)30194-5

DOI: <https://doi.org/10.1016/j.jmat.2020.08.006>

Reference: JMAT 346

To appear in: *Journal of Materiomics*

Received Date: 29 April 2020

Revised Date: 4 August 2020

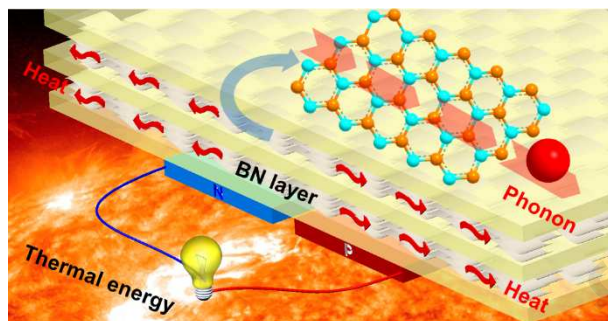
Accepted Date: 17 August 2020

Please cite this article as: Wang J, Liu D, Li Q, Chen C, Chen Z, Naebe M, Song P, Portehault D, Garvey CJ, Golberg D, Lei W, Nacre-bionic nanocomposite membrane for efficient in-plane dissipation heat harvest under high temperature, *Journal of Materiomics* (2020), doi: <https://doi.org/10.1016/j.jmat.2020.08.006>.

This is a PDF file of an article that has undergone enhancements after acceptance, such as the addition of a cover page and metadata, and formatting for readability, but it is not yet the definitive version of record. This version will undergo additional copyediting, typesetting and review before it is published in its final form, but we are providing this version to give early visibility of the article. Please note that, during the production process, errors may be discovered which could affect the content, and all legal disclaimers that apply to the journal pertain.

© 2020 The Chinese Ceramic Society. Production and hosting by Elsevier B.V. All rights reserved.

## Graphical Abstract



## **Nacre-bionic nanocomposite membrane for efficient in-plane dissipation heat harvest under high temperature**

Jiemin Wang<sup>a</sup>, Dan Liu<sup>a\*</sup>, Quanxiang Li<sup>a</sup>, Cheng Chen<sup>a</sup>, Zhiqiang Chen<sup>a</sup>, Minoo Naebe<sup>a</sup>, Pingan Song<sup>b\*</sup>, David Portehault<sup>c</sup>, Christopher J. Garvey<sup>d</sup>, Dmitri Golberg<sup>c</sup>, Weiwei Lei<sup>a\*</sup>

<sup>a</sup>Institute for Frontier Materials, Deakin University, Waurn Ponds Campus, Locked Bag 20000, Victoria 3220, Australia.

<sup>b</sup>Center for Future Materials, University of Southern Queensland, Toowoomba, 4350, Australia.

<sup>c</sup>Sorbonne Université, CNRS, Laboratoire de Chimie de la Matière Condensée de Paris (CMCP), 4 place Jussieu, F-75005, Paris, France

<sup>d</sup>Australia Nuclear Science and Technology Organization (ANSTO), Sydney, New South Wales 2232, Australia.

<sup>e</sup>Centre for Materials Science and School of Chemistry and Physics, Queensland University of Technology (QUT), Brisbane, QLD 4001, Australia

### **\*Corresponding author**

Dr. Dan Liu; Dr. Weiwei Lei

E-mail: [dan.liu@deakin.edu.au](mailto:dan.liu@deakin.edu.au); [weiwei.lei@deakin.edu.au](mailto:weiwei.lei@deakin.edu.au)

Dr. Pingan Song

E-mail: [pingsong@gmail.com](mailto:pingsong@gmail.com)

**Keywords:** boron nitride nanosheets, nanocomposite membrane, nacre-biomimetic, high temperature heat spreader, in-plane dissipation heat

**Abstract:**

Waste heat management holds great promise to create a sustainable and energy-efficient society as well as contributes to the alleviation of global warming. Harvesting and converting this waste heat in order to improve the efficiency is a major challenge. Here we report biomimetic nacre-like hydroxyl-functionalized boron nitride (BN)-polyimide (PI) nanocomposite membranes as efficient 2D in-plane heat conductor to dissipate and convert waste heat at high temperature. The hierarchically layered nanostructured membrane with oriented BN nanosheets gives rise to a very large anisotropy in heat transport properties, with a high in-plane thermal conductivity (TC) of  $51 \text{ W m}^{-1} \text{ K}^{-1}$  at a temperature of  $\sim 300 \text{ }^\circ\text{C}$ , 7314% higher than that of the pure polymer. The membrane also exhibits superior thermal stability and fire resistance, enabling its workability in a hot environment. In addition to cooling conventional exothermic electronics, the large TC enables the membrane as a thin and 2D anisotropic heat sink to generate a large temperature gradient in a thermoelectric module ( $\Delta T = 23^\circ\text{C}$ ) through effective heat diffusion on the cold side under  $220^\circ\text{C}$  heating. The waste heat under high temperature is therefore efficiently harvested and converted to power electronics, thus saving more thermal energy by largely decreasing consumption.

## 1. Introduction

Recent years have witnessed the growing power density of electronic devices, which results in excessive thermal energy accumulation. The concomitant temperature increase can damage the products and even raise safety risks, such as fire or explosion [1]. Other sources of heat, like furnaces in steel factories generate also large amounts of waste heat that is directly released into the surrounding atmosphere. Heat dissipating materials are usually required to enable the cooling of these electronics and furnaces [2-3]. In this context, hexagonal boron nitride (BN) nanosheets-based heat sinks have been largely investigated owing to the high thermal conductivity (TC) and chemical stability [4-8]. BN based nanocomposites can also be conveniently processed as a flexible membrane to optimize conformal coating of the heat source, and then fasten heat diffusion from the hot source to the membrane edges along the in-plane direction, thereby decreasing the hot source temperature and dissipating the accumulated heat. This cooling process, however, gives rise to a waste of excessive dissipated thermal energy. Despite great advances in the development of heat harvest thermoelectric devices, they are restricted to operation at relatively low-grade temperatures (<100 °C) [9]. Therefore, the design of high-performance thermally conductive membranes remains a major challenge to dissipate as well as efficiently harvest high-temperature waste heat above 200 °C.

Due to its structural configuration, the most efficient way to conduct heat within a membrane is to maximize the in-plane TC while maintaining low transverse TC, hence achieving a large TC anisotropic ratio. Previous researches have reported BN/polymer nanocomposite membranes with biomimetic nacre-like structure for effective thermal diffusion [4, 5, 7, 8, 10, 11]. The nacre-like laminated structure is based on the lateral alignment of platelets within a polymer matrix in a “brick-and-mortar” scheme. It enables heat conduction along the

nanosheet layers, resulting in large in-plane thermal conductivity. The nacre mimics membranes also exhibit flexibility and toughness, fully applicable to soft electronics. However, the low thermal stability and moisture sensitivity of polymers such as poly vinyl alcohol (PVA) [4,10,11], poly diallyldimethylammonium chloride (PDDA) [5] and cellulose [7,8] have hindered the practical use to these membranes above 200 °C and in humid atmosphere. Some thermostable polymers such as polyimide (PI) have been considered to reach higher temperatures [12, 13]. Nevertheless, to date, nacre-like nanocomposites based on BN and PI remain intractable to achieve *via* vacuum filtration (VAF) because of the poor compatibility between BN and PI as well as the poor solubility of PI in water. Moreover, traditional mixing and coating methods result in relatively low in-plane thermal conductivity [12, 13]. Overall, no thermally conductive yet electrically insulating nacre-like membrane has been delivered to operate in harsh temperature conditions, above 200 °C, with satisfying high thermal conductivity ( $>30 \text{ W m}^{-1} \text{ K}^{-1}$ ). Hence, the design of nacre-like BN/PI nanocomposites membranes is critical to combine high thermal conductivity and thermal stability.

Here, we design freestanding and nacre-like BN nanosheet/PI (BN-PI) nanocomposite membranes by using the VAF assembly of hydroxyl functionalized BN nanosheets and a water-soluble modified precursor of PI, followed by thermal treatment. Besides significant improvements in mechanical performances and flame resistance, the membranes exhibit considerable in-plane TCs at 200 °C ( $35\text{-}49 \text{ W m}^{-1} \text{ K}^{-1}$ ) and at 300 °C ( $36\text{-}51 \text{ W m}^{-1} \text{ K}^{-1}$ ) with 30-70 wt% BN, respectively, allowing efficient anisotropic thermal regulation in a wide temperature range. In order to dissipate and harvest the redundant heat, the membrane was connected to the cold side of a thermoelectric (TE) module. Unlike conventional exothermic electronics with low heating temperature ( $<100 \text{ °C}$ ), the TE module can be heated to maximum 220°C, thereby benefiting our membrane for cooling applications from high

temperatures. Thanks to the ability of the BN-PI membrane to act as an efficient and thermo-stable heat sink through in-plane heat conduction, the TE module could reach larger temperature gradient ( $\Delta T$ ) between the hot and cold sides, and achieve larger thermoelectric energy conversion efficiency with more thermal energy conservation. This work then offers an original methodology to design a biomimic thermo-anisotropic membrane as high temperature heat spreader for cost-effective harvesting and conversion of waste heat.

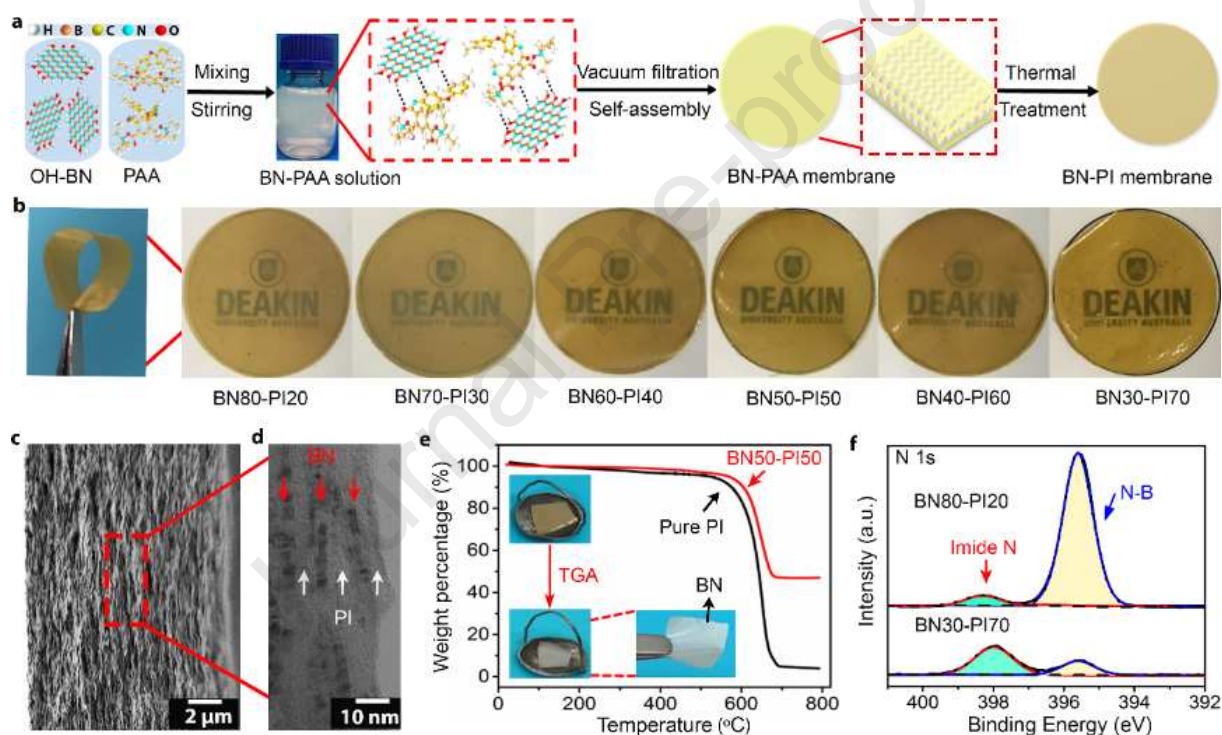


**Figure 1.** Fabrication and structural characterization of nacre-like BN-polyimide nanocomposite membranes. (a) Scheme of the fabrication process of the membranes. (b) Optical images of the membranes with different BN weight loadings. The use of the logo is permitted from the Institute of Frontier Materials, Deakin University. (c) SEM and (d) TEM images of the cross-sectional morphology of a BN50-PI50 membrane. (e) TGA traces of BN50-PI50 and pure PI membranes. The insets in (e) display the optical images of the

nanocomposite membrane before and after TGA tests. (f) N 1s region of the XPS spectra of BN80-PI20 and BN30-PI70.

## 2. Experimental

**2.1 Material synthesis:** *Preparation of functional boron nitride (BN) nanosheets.* At first, h-BN (Momentive Performance Materials, Inc.) and D-glucose (Sigma-Aldrich) were mixed and milled in a planetary ball mill (Pulverisette 7, Fritsch) at a rotation speed of 500 r.p.m. for 20 h. The achieved powders were dissolved in water and dialyzed for 7 days to remove the D-glucose, producing stable aqueous dispersions of BN nanosheets [14].

*Preparation of water-soluble polyimide (PI) precursor.* The 4, 4'-diaminodiphenyl ether (4,4'-ODA, Sigma-Aldrich), pyromellitic dianhydride (PMDA, Sigma-Aldrich) and triethylamine (TEA) (Sigma-Aldrich) were used to synthesize (amic acid) (PAA) solution, as previously reported [6,15].

*Preparation of freestanding BN-PI membranes.* BN-PI membranes were fabricated by water vacuum-assisted filtration and thermal crosslinking. The aqueous solution of BN nanosheets was mixed with PAA solution at first, and then the mixtures were magnetically stirred for 1 h. Then the mixtures were filtered under vacuum. These BN-PAA membranes can be readily peeled off from the polyethylene membrane and retain their freestanding state. After these procedures, the films were thermally cross-linked in a tube furnace under N<sub>2</sub> protection at 80 °C, 150 °C, 170 °C for 1 h, respectively, and finally at 300 °C for 2 hrs.

**2.2 Material Characterization:** XRD measurements were processed on a PANalytical X'Pert apparatus with Cu K $\alpha$  radiation. The FTIR spectra were measured using a Nicolet 7199 FTIR spectrometer. XPS analysis was performed on an Kratos AXIS Nova instrument

with Al K $\alpha$  X-ray as the excitation source. SEM imaging was carried out using a Zeiss Supra 55 VP SEM instrument. TEM and HRTEM imaging was conducted on a JEOL 2100F microscope operating at 200 kV. The mechanical measurements were performed by means of an Instron 30 KN tensile tester on a 50 N load cell with a loading rate of 5 mm/min. The modeling was processed by COMOSOL Multiphasics software under steady-state. The thermal weight losses were measured using TGA on a TA Instruments Q50 at a heating rate of 10 °C min<sup>-1</sup> from room temperature to 800 °C under air flow. The specific heat was measured by using the differential scanning calorimetry (DSC Q200, TA Instruments). Here, the heat capacity of a nanocomposite was calculated using the equation:  $C_p = C_{pf}\Phi + C_{pm}(1-\Phi)$  [4-6], where  $C_p$  is the specific heat capacity of the nanocomposite and  $C_{pf}$  is the specific heat capacity of the filler (BN), and  $C_{pm}$  is the specific heat capacity of the polymer (PI), whereas  $\Phi$  represents the volume fraction of BN. The in-plane and out-of-plane thermal diffusivity of nanocomposite membranes were measured from 30-300 °C with an LFA 457 analyzer (NETZSCH, Germany). The thermal conductivities of the nanocomposite membranes were calculated according to the equation  $TC = \alpha \times \rho \times C$  (Table S2), where  $\alpha$ ,  $\rho$ , and  $C$  correspond to the thermal diffusivity, density, and specific heat capacity of the nanocomposites. The flame retardancy test was performed on BN-PI and pure PI membranes separately. The fire from a gas burner was applied to the tested membranes for 60 s and then removed. The thermoelectric (TE) measurements were performed by placing the membrane on the cold side surface of a commercial TE module (30 mm x 30 mm, 128 pairs of p-n junction with Bi<sub>2</sub>Te<sub>3</sub> as materials). Then, a thermal conductive glue ( $TC \sim 4.5 \text{ W m}^{-1} \text{ K}^{-1}$ ) was coated on the cold side of TE module to paste the membrane. Meanwhile, the TE module was also placed on a Cu column with hot stage heating. The voltage and current values were measured by a multimeter and the temperatures of cold side and hot side were detected by 2

digital thermometers. The maximum heating temperature was not more than 220 °C, otherwise the TE module would malfunction due to high temperature.

### 3. Results and discussion

The fabrication of the membranes is illustrated in Figure 1a. Firstly, hydroxylated BN nanosheets (OH-BN) were produced by ball milling (Figure S1a) [14]. These BN nanosheets possess 100-300 nm lateral size, 1-2 nm thickness and hydroxyl-functionalized surfaces, which enable water dispersibility (Figure S1b-e), hence vacuum filtration processing. Secondly, we prepared the aqueous solution of polyamic acid (PAA), the precursor of polyimide PI [15]. The BN suspension and aqueous solution of PAA were then mixed at arbitrary ratios to form a homogeneous mixture without visible aggregation. We assume that multiple nanosheets-polymer interactions may arise, such as hydrogen-bonding,  $\pi$ - $\pi$  stacking, and electrostatic repulsions, and then pack the BN sheets and PAA in water. Afterwards, the yellowish suspension was obtained (Figure S2). The final free-standing yellow BN-PI nanocomposite membranes were readily prepared by VAF followed by thermal treatment. BN-PI nanocomposite membranes with various BN contents could be conveniently produced by varying the concentrations of the components in the aqueous suspension. The weight contents of BN evaluated by thermogravimetric analysis (TGA) were consistent with the targeted mass ratios (Figure S3). These ratios set at 80, 70, 60, 50, 40, and 30 wt.% for membranes were denoted as BN80-PI20, BN70-PI30, BN60-PI40, BN50-PI50, BN40-PI60 and BN30-PI70, respectively. As shown in Figure 1b, the resultant BN-PI membranes are translucent and flexible even at high BN loading, despite the intrinsic brittleness of BN nanosheets [14]. Scanning electron microscopy (SEM) and transmission electron microscopy (TEM) images (Figure 1c and d) highlight the layered nanostructure of the membrane BN50-

PI50. On the surface area, the BN nanosheets are homogeneously distributed within the PI matrix (Figure S4). Meanwhile, cross-section images confirm the nacre-like lamellar “brick-and-mortar” structure (Figure 1c-d and Figure S5). As shown in the Figure 1e inset, the white BN membranes maintain their original shape even after experiencing heat treatment from 25°C to 800 °C in air, thus indicating excellent structure stability and thermal stability. The SEM images of the net BN membrane (Figure S6) after calcination show the parallel stacking of BN lamellae with PI burnt-out spaces, providing another evidence for the layered self-assembly of the nanocomposite membrane. The chemical composition was investigated by X-ray photoelectron spectroscopy (XPS) (Figure 1f and Figure S7). The N-B peak (~398 eV, Figure 1f) [14] dominates in the BN80-PI20 membrane, while the relatively strong imide N peak (~400.5 eV, Figure 1f) [15, 16] appears in the BN30-PI70 in the N 1s spectrum, confirming the ability to tune the ratio between BN and PI. The results are further evidenced by X-ray diffraction (XRD) (Figure S8a), small-angle X-ray scattering (SAXS) (Figure S8b) and Fourier transform infrared spectroscopy (FTIR) (Figure S9).

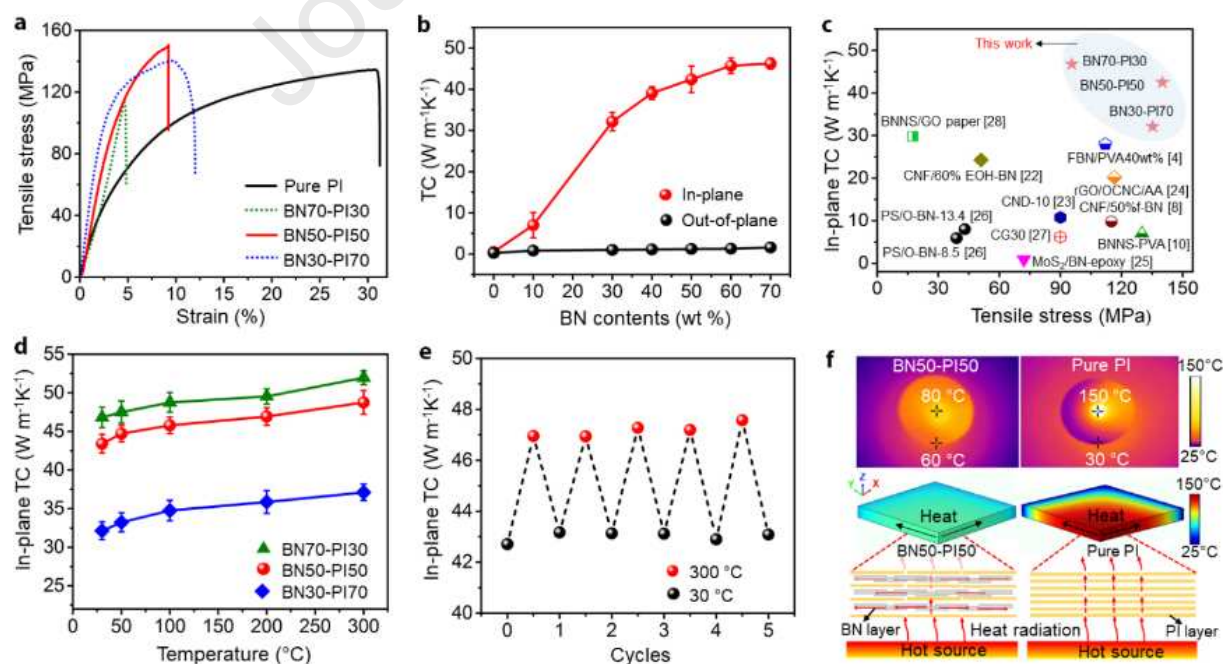


**Figure 2.** Mechanical and thermal conduction properties of the BN-PI membranes. (a)

Tensile stress measurements. (b) In-plane and out-of-plane thermal conductivities (TCs) with different BN weight loadings. (c) Performance chart of membranes integrating in-plane TC and tensile stress. (d) Temperature-dependent TCs of BN-PI membranes. (e) Temperature cyclability of the BN50-PI50 membrane. (f) In-plane heat dissipation mechanism (IR imaging and steady simulation model) of BN-PI membrane (left) and pure PI membrane (right).

The mechanical properties of the nanocomposite membranes were then investigated (Figure 2a, Figure S10 and table S1). The BN50-PI50 membrane exhibits the maximum tensile stress with a value of  $\sim 140$  MPa and a Young's modulus of  $\sim 2.53$  GPa (Figure S10 a, b and c). These values are superior to those of BN-PVA and BN-PDDA membranes reported previously [4, 5]. The enhancement of the mechanical properties of the materials shown herein may arise from both the superior mechanical characteristics of PI and the homogeneous distribution of the BN nanosheets. Under tensile loads, the artificial nacre-like architecture enables longitudinal transfer of the force along the nanosheets and through the polymer component, which then jointly undertake the load [17-21]. Not surprisingly, the mechanical properties are optimized for an intermediate BN content, here for BN50-PI50 at 50 wt. % BN. Below this amount, the BN sheets are not in sufficient amount to enhance the mechanical properties, whereas an excessive BN content can lead to reduced extensibility and toughness (Figure S10d). We then measured the thermal conductivity properties. As expected, the in-plane TC increases with the BN content (Figure 2b), leading to a value of  $47.8 \text{ W m}^{-1} \text{ K}^{-1}$  for BN70-PI30. Even at a low 30 wt. % (17.7 vol.%) BN loading (BN30-PI70 membrane), the in-plane TC is enhanced with a value as high as  $32.1 \text{ W m}^{-1} \text{ K}^{-1}$ , about 7314% increase compared to the pure polymer. In contrast, the out-of-plane TC values maintain small values. Therefore, the high in-plane thermal conductivity of the BN nanosheets is attributed to the nacre-like structure: the aligned sheets build a heat path allowing rapid heat dissipation in-

plane rather than out-of-plane, resulting in a significant thermal anisotropy [4, 5, 22-24]. To compare the thermal and mechanical properties, we plotted both tensile stress and in-plane TCs in a performance chart in Figure 2c. Notably, for all BN contents from 30 wt.% to 70 wt.%, the BN-PI membranes show superior thermal conduction and mechanical properties than other membranes based on BN and other 2D materials, such as graphene and MoS<sub>2</sub> [4, 8, 10, 22-28]. In addition, the highest temperatures that membranes can withstand determine their practical applications in hot environments. However, previously reported polymer/BN composites cannot maintain their thermal conductivity above 125-160 °C [4, 5, 7, 8, 10, 11]. Impressively, the BN-PI membranes described herein retain large TCs at temperatures up to 300 °C (36-51 W m<sup>-1</sup> K<sup>-1</sup> with 30-70 wt.% BN loading) (Figure 2d). Regardless of subtle fluctuations due to the balance effect of Umklapp phonon scattering and reduced Kapitza resistance [7], the TC measured for the BN-PI membranes increases by less than 10% from 30 °C to 300 °C, thus showing stable enough thermal properties for applications at high temperatures. Furthermore, TC shows only a slight change upon 5 heating/cooling alternative cycles between 30°C to 300 °C (Figure 2e), demonstrating high cycle durability.

To further understand the heat conduction mechanism, an infrared (IR) thermal camera was employed to record the temperature distribution in the membrane in a steady-state condition (Figure 2f). The BN50-PI50 membrane with optimal mechanical and thermal performances was chosen for these measurements. The membrane was put on a hot iron head at 200 °C. A blurry hot spot appears with low temperature on its surface centre (80 °C). Moreover, the temperature is also uniformly distributed from the centre to the edge of the membrane (60 °C). On the contrary, the pure PI membrane shows a focused bright spot in its centre, reaching 150 °C, while the edge temperature is as low as 30 °C. The high in-plane TC and large thermal conductive anisotropy of the BN-PI membrane enable the heat flux to rapidly spread from the hot spot to the edge along the in-plane direction, leading to efficient cooling with a

uniform temperature distribution. Steady-state simulations also confirm the homogeneous temperature distribution within the BN50-PI50 membrane, originating from efficient in-plane heat dissipation (Figure S11). Whereas intensive heat accumulates in the centre for the pure PI membrane, causing a strong temperature gradient.

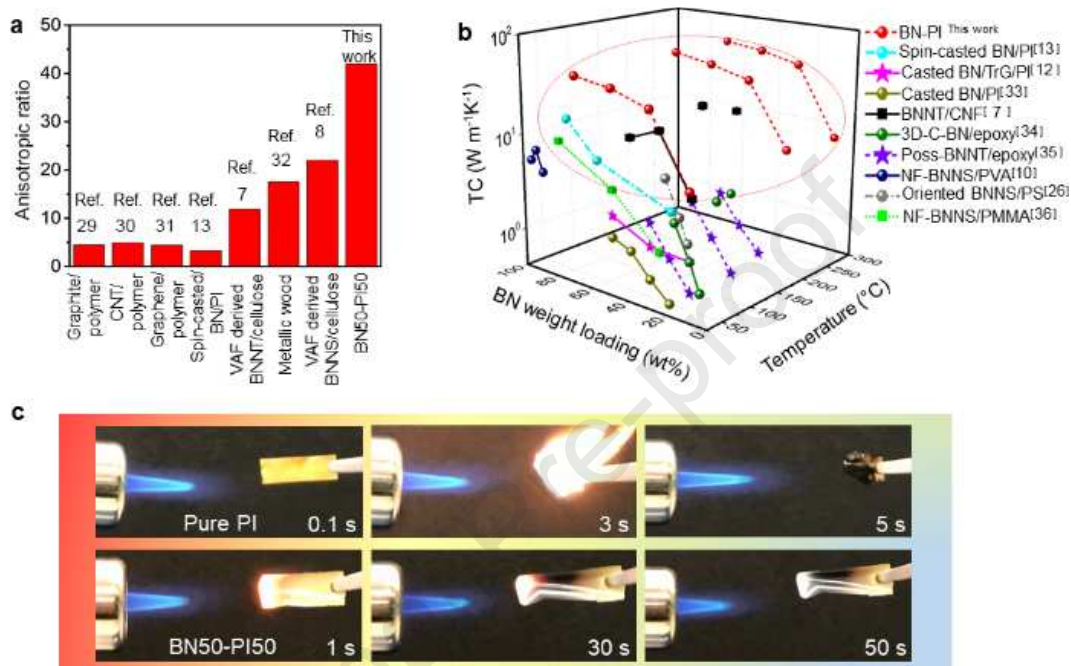


**Figure 3.** The high temperature thermo-anisotropy and flame resistance. (a) Comparison of anisotropic thermal conduction ratios among various heat sink materials. (b) Comparison of TCs over a wide temperature range with different BN contents. (c) Flame resistance test between pure PI and BN50-PI50 membrane.

To further verify the anisotropic thermal property, the anisotropic thermal conduction ratios ( $TC_{in-plane}/TC_{out-of-plane}$ ) among various heat sink materials are displayed in Figure 3a. Obviously, BN50-PI50 possesses a large anisotropic ratio of 42, which is greater than that for graphite/polymer, CNT/polymer composites and metallic wood [29-32]. Besides, the nanocomposite membrane with the lamellae-based, nacre-like structure has a greater anisotropy than films prepared via blade coating [7, 8, 13]. This result shows that the bio-

inspired construction can orient the phonon transport by aligning the thermally conductive BN sheets along the plane of the membrane. Therefore, the in-plane BN lamellae not only determines the great mechanical property but also guarantees the excellent anisotropic thermal conduction performances. Furthermore, we also compared the TC values during a wide temperature range (25-300°C) with different BN contents (Figure 3b). It is important that the BN-PI membranes presented large TC values of an order of magnitude higher than other BN-based thermal conductive composites for all temperatures [7, 12, 13, 26, 33-36]. In addition, we also observed excellent flame-resistance of the as-designed membranes (Figure 3c). The pure PI membrane was combustible and burnt out in 5 s when it was close to the flame. Nevertheless, for the nanocomposites, the fire resistance capacity was improved with the BN contents (Figure S12). When the BN weight content reaches 50 wt.% or more, the nanocomposite membranes could maintain their initial shapes within around 1 min. Therefore, such a unique performances combination enables the BN-PI membrane to serve as a promising 2D heat sink for thermal manipulation at high temperature up to 300 °C as well as validating practical workability in some extreme conditions, such as fire circumstances.

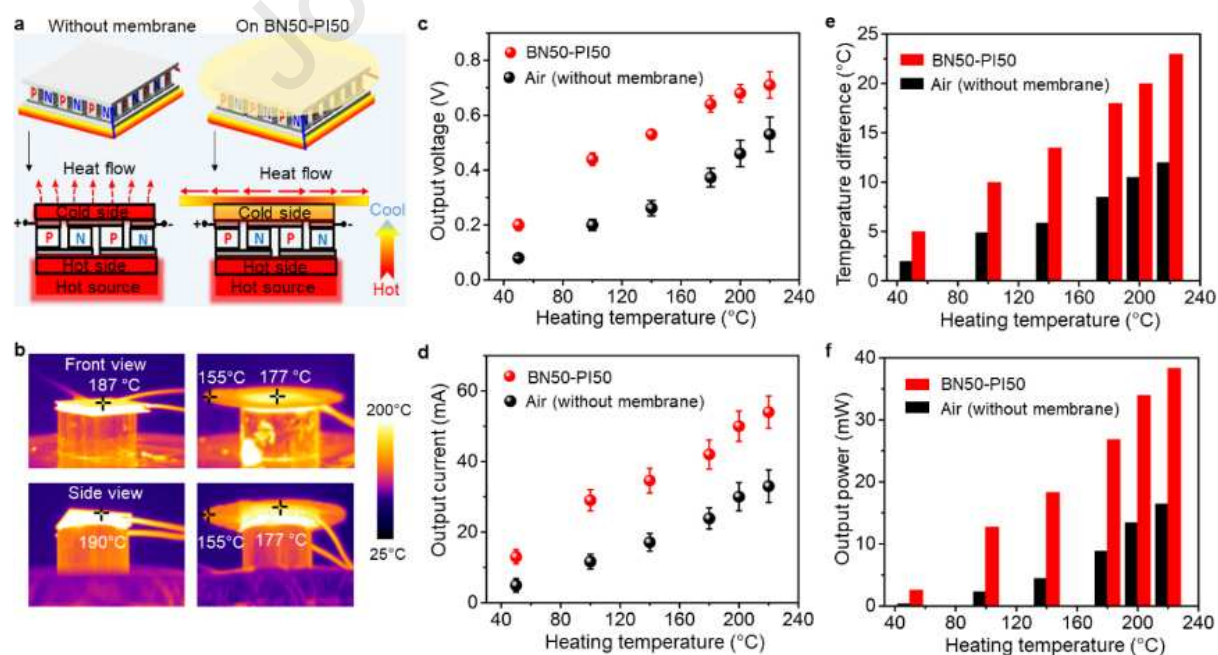


**Figure 4.** The applications of BN-PI nanocomposite membranes as a heat sink for thermal energy conversion. (a) Scheme of the design concept and mechanism for natural air-cooled (left) and BN50-PI50 membrane-loaded (right) TE module. (b) Corresponding temperatures recording by IR imaging for 220 °C heating. (c) Voltage generated at different heating temperatures. (d) Current generated at different heating temperatures. (e) Temperature difference between the hot and cold sides of the TEG generators at different heating temperatures. (f) Power generated at different heating temperatures.

In addition to cooling the conventional electronics such as (light-emitting diode) LED bubbles with working temperature less than 100°C [5-7], the high cooling efficiency of BN-PI membranes could advantageously contribute to the performances of thermoelectric generators (TEGs) at higher temperatures (>200°C) by using the membranes as heat sinks. In order to achieve great thermal-to-electricity conversion in TEGs, the temperature difference between the cold ( $T_{\text{cold}}$ ) and hot ( $T_{\text{hot}}$ ) ends must be maximized [15, 37]. Heat sinks enable maintaining low  $T_{\text{cold}}$  by dissipating heat. Most of them are composed of metals or carbon materials that are bulky and not electrically insulating. They also tend to generate heat by the photothermal effect, especially when exposed to outdoor environment [38-40]. Therefore, the 2D lightweight BN-PI membranes described herein, with unprecedented combination of large in-plane TCs and high temperature workability, may serve as efficient next-generation heat sinks to harvest waste heat with TEGs. We designed a TEG (Figure 4a) based on the BN50-PI50 membrane to evaluate the feasibility of heat harvesting and conversion. A large freestanding membrane with diameter of 65 mm was first fabricated (Figure S13) according to the process described in Figure 1a. It was then assembled on the cold side of a commercial TE module (30 mm in length and width). The as-obtained TEG was placed on a Cu column (hot source) heated by a hot stage. The whole experiment was conducted in the steady-state achieved after at least 10 min of operation. The corresponding temperature distributions from

front and side views of the TEG (without or with membrane loaded) were measured by IR imaging (Figure 4b). When the temperature of the hot stage reached 220 °C, the central and edge temperatures of the BN50-PI50 membrane were 177 °C and 155°C, respectively. In contrast, the temperature of the naturally air-cooled device without membrane rose to ~190°C in the centre. Notably, the pure PI membrane of the same size showed similar or even higher temperatures under air cooling since the pure polymer membrane is thermo-insulating; this results in the worse heat dissipation under air cooling.<sup>15</sup> Hence, we did not present the results for a pure PI membrane.. To further validate this observation, we also used two digital thermometers to detect the temperatures of the cold and hot sides of the TEG (Figure S14). The temperature gradient expands from 12 °C to 23 °C for the naturally cooled and the membrane-modified device, respectively. Although the temperatures measured by the point-thermometer differ by few degrees from those evaluated by IR imaging, the trends and orders of magnitude are identical: they clearly demonstrate that the BN50-PI50 heat sink membrane effectively dissipates heat and double the temperature gradient. As a result, the thermoelectric conversion efficiency of the TEG should be strongly increased. Figure 4c and d display the Seebeck output voltage (V) and current (I) with and without BN50-PI50 heat sink membrane at different heating temperatures. As expected, the membrane loaded TE device yields larger voltages and currents. Although the membrane can work at 300 °C, we still set the upper limit of the heating temperature to 220 °C, because of the upper temperature limitation of the commercial TE module. When the hot stage was heated to 220 °C, we could achieve a voltage of ca. 0.71 V and a current of 54 mA, i.e. 34% and 40% enhancements versus the membrane-free device. These results validate the suitability of the BN50-PI50 membrane to enhance heat harvesting and conversion with thermoelectric generators, hence highlighting the high temperature availability. As presented in Figure 4e,  $\Delta T$  increases with the hot side temperature. For the BN50-PI50 membrane-loaded TEG,  $\Delta T$  is nearly twice that under air-

cooling, indicating efficient heat dissipation. To confirm the temperature gradient measurement (Figure S15), we calculated the expected Seebeck voltages of the TEG for such temperature gradients (Figure S16). The measured values fit well with the expected ones, despite a minor deviation at larger  $\Delta T$  that is reasonable due to the not regulated ambient surroundings. Encouragingly, the maximum output power from the BN50-PI50-loaded TEG reaches 38.3 mW (Figure 4f), i.e. 132 % higher than for the air-cooled device (16.5 mW), indicating that additional 21.8 mW power is generated by the BN50-PI50-loaded TEG at 220 °C hot stage heating. Hence, apart from efficient cooling, such temperature differences enable extra power generation. Furthermore, previous membrane cooling efficiency measurements mainly relied on either IR images or digital thermometers [4, 6]. In contrast, this conceptual design provides a more practical approach for evaluating the practical heat dissipation ability of a thermal sink.



**Figure 5.** Tandem connection for practical cooling from high temperature and thermal energy utilization. (a) The scheme of BN50-PI50 for efficient high temperature heat dissipation and

practical thermal energy conversion. (b) The optical picture of practical tandem of an air-cooling based TE module. (c) The optical picture of a practical tandem of BN50-PI50 loaded TE module.

To further enable the practicability for high temperature cooling and waste heat conversion, we then connected 3 TE modules in series (Figure 5a) and no any voltage amplifier or power charging sub-assembly were introduced. Interestingly, the naturally cooled TEG without the heat spreader yielded a total output voltage of only 1.66 V, even under maximum heating temperature at 220 °C (Figure 5b). By comparison, the assembly of BN50-PI50-membrane loaded TEGs delivers a total output voltage of 1.92 V that is enough to steadily drive a LED bubble (working voltage 1.8 V) and a calculator (Figure 5c and Figure S17, Videos S1 and S2). This high voltage was reached far below the maximum operation temperature (220 °C), at 180°C. This should reduce the cost of the whole energy conversion process. These encouraging results attributed to the efficient cooling of the thermo-anisotropic BN50-PI50 heat sink membrane, where the nacre-like BN and PI nanostructure dissipates heat in the membrane plane. Meanwhile, the high thermal stability of BN and PI allows for workability in such a hot condition for more cost-effective power conversion, which is applicable for in-plane waste heat utilization under high temperature.

#### **4. Conclusions**

In summary, we have successfully designed bio-inspired nacre-like freestanding boron nitride-polyimide nanocomposite membranes. The laminated layered structure of the nanocomposite not only improves the mechanical performances, but also provides superior thermal conductivity along the plane of the membranes. Additionally, the membrane features fire-resistance and high thermal stability in a wide temperature range (30-300 °C), combined with great thermo-anisotropy. These characteristics provide the membrane with high

potential for use as a 2D heat sink to cool a variety of electronic components working at high temperatures. For instance, the biomimetic membrane in this work can be highly effective for heat dissipation on the cold side of the TE module even under 220°C heating, hence improving the planar thermal-to-electrical energy conversion. Therefore, our work provides an effective strategy to fabricate high temperature thermal spreader for efficient waste in-plane heat harvest and conversion.

### **Conflicts of interest**

The authors declare that they have no known competing financial interests or personal relationships that could have appeared to influence the work reported in this paper.

### **Supporting Information**

Supporting Information is available from the ELSEVIER or from the author.

### **Funding**

This work was financially supported by the Australian Research Council Discovery Program (DP190103290) and Australian Research Council Discovery Early Career Researcher Award scheme (DE150101617 and DE140100716). We also thank the Australian Synchrotron for the SAXS/WAXS beamline (Beam time ID: M13292). D.G. is grateful to the Australian Research Council Laureate Fellowship FL160100089 and QUT Project No. 323000-0355/51.

### **References**

- [1] R. Ma, Z. Zhang, K. Tong, D. Huber, R. Kornbluh, Y. Ju, Q. Pei, *Science*, 357 (2017) 1130-1134.
- [2] H. Song, J. Liu, B. Liu, J. Wu, H. M. Cheng, F. Kang, *Joule*, 2 (2018) 442-463.

- [3] Y. Zhang, Y. Heo, Y. Son, I. In, K-H. An, B-J. Kim, S-J. Park, *Carbon*, 142(2019) 445-460.
- [4] J. Wang, Y. Wu, Y. Xue, D. Liu, X. Wang, X. Hu, Y. Bando, W. Lei, *J. Mater. Chem. C*, 6 (2018) 1363-1369.
- [5] Y. Wu, Y. Xue, S. Qin, D. Liu, X. Wang, X. Hu, J. Li, Y. Bando, D. Golberg, Y. Chen, Y. Gogotsi, W. Lei, *ACS Appl. Mater. Interfaces*, 9 (2017) 43163-43170.
- [6] J. Wang, Q. Li, D. Liu, C. Chen, Z. Chen, C. Yang, J. Hao, Y. Li, J. Zhang, M. Naebe, W. Lei, *Nanoscale*, 10 (2018) 16868-16872.
- [7] X. Zeng, J. Sun, Y. Yao, R. Sun, J. Xu, C. P. Wong, *ACS Nano*, 11 (2018) 5167-5178.
- [8] K. Wu, J. Fang, J. Ma, R. Huang, S. Chai, F. Chen, Q. Fu, *ACS Appl. Mater. Interfaces*, 9 (2017) 30035-30045.
- [9] L. Zhang, T. Kim, N. Li, T. Kang, J. Chen, J. Pringle, M. Zhang, A. Kazim, S. Fang, C. Haines, D. Al-Masri, B. Cola, J. Razal, J. Di, S. Beirne, D. MacFarlane, A. Martin, S. Mathew, Y. Kim, G. Wallace, R. Baughman, *Adv. Mater.*, 29 (2017) 1605652.
- [10] X. Zeng, L. Ye, S. Yu, H. Li, R. Sun, J. Xu, C. P. Wong, *Nanoscale*, 7 (2015) 6774-6781.
- [11] Y. Yao, X. Zeng, R. Sun, J. Xu, C. P. Wong, *ACS Appl. Mater. Interfaces*, 8 (2016) 15645-15653.
- [12] M. H. Tsai, I. H. Tseng, J. C. Chiang, J. Li, *ACS Appl. Mater. Interfaces*, 6 (2014) 8639-8645.
- [13] M. Tanimoto, T. Yamagata, K. Miyata, S. Ando, *ACS Appl. Mater. Interfaces*, 5 (2013) 4374-4382.
- [14] W. Lei, N. V. Mochalin, D. Liu, S. Qin, Y. Gogotsi, Y. Chen, *Nat. Commun.*, 6 (2015) 8849.
- [15] J. Wang, D. Liu, Q. Li, C. Chen, Z. Chen, S. Fakhrohoseini, M. Naebe, P. Song, X. Wang, W. Lei, *ACS Nano*, 13 (2019) 7860-7870.
- [16] W. Ha, A. Choudhury, T. Kamal, D. Kim, S. Y. Park, *ACS Appl. Mater. Interfaces*, 4 (2012) 4623-4630.
- [17] Z. Ling, C. E. Ren, M. Zhao, J. Yang, J. M. Giammarco, J. Qiu, M. W. Barsoum, Y. Gogotsi, *Proc. Natl. Acad. Sci.*, 11 (2014) 16676-16681.
- [18] J. Zhu, H. Zhang, N. Kotov, *ACS Nano*, 7 (2013) 4818-4829.
- [19] N. Kotov, *Natl. Sci. Rev.*, 4 (2017) 284-285.
- [20] S. Wan, Y. Li, J. Mu, A. Aliev, S. Fang, N. Kotov, L. Jiang, Q. Cheng, R. Baughman, *Proc. Natl. Acad. Sci.*, 21 (2018) 5359-5364.
- [21] P. Song, J. Dai, G. Chen, Y. Yu, Z. Fang, W. Lei, S. Fu, H. Wang, Z. Chen, *ACS Nano*,

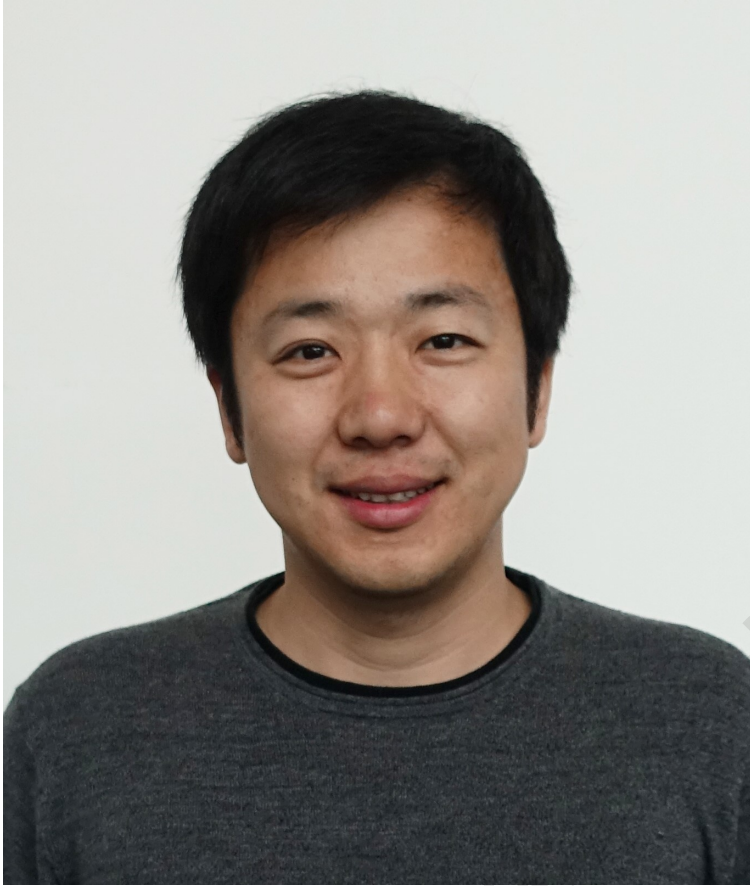
- 12 (2018) 9266-9278.
- [22] K. Wu, P. Liao, R. Du, Q. Zhang, F. Chen, Q. Fu, *J. Mater. Chem. A*, 6 (2018) 11863–11873.
- [23] N. Song, S. Cui, X. Hou, P. Ding, L. Shi, *ACS Appl. Mater. Interfaces*, 9 (2017) 40766-40773.
- [24] H. Zeng, J. Wu, Y. Ma, Y. Ye, J. Liu, X. Li, Y. Wang, Y. Liao, X. Luo, X. Xie, X. Mai, *ACS Appl. Mater. Interfaces*, 10 (2018) 41690-41698.
- [25] H. Ribeiro, J. Trigueiro, W. Silva, C. Woellner, P. Owuor, A. Chipara, M. Lopes, C. Tiwary, J. Pedrotti, C. Salvatierra, J. Tour, N. Chopra, I. Odeh, G. Silva, P. M. Ajayan, *ACS Appl. Mater. Interfaces* (2017) 10.1021/acsami.7b09945.
- [26] X. Wang, P. Wu, *ACS Appl. Mater. Interfaces*, 9 (2017) 19934–19944.
- [27] N. Song, D. Jiao, P. Ding, S. Cui, S. Tang, L. Shi, *J. Mater. Chem. C*, 4 (2016) 305-314.
- [28] Y. Yao, X. Zeng, F. Wang, R. Sun, J. Xu, C. P. Wong, *Chem. Mater.*, 28 (2016) 1049–1057.
- [29] X. Tian, M. E. Itkis, E. B. Bekyarova, R. C. Haddon, *Sci. Rep.*, 3 (2013) 01710.
- [30] J. G. Park, Q. Cheng, J. Lu, J. Bao, S. Li, Y. Tian, Z. Liang, C. Zhang, B. Wang, *Carbon*, 50 (2012) 2083-2090.
- [31] J. Gong, Z. Liu, J. Yu, D. Dai, W. Dai, S. Du, C. Li, N. Jiang, Z. Zhan, C. T. Lin, *Compos. Part A Appl. Sci. Manuf.*, 87 (2016) 290-296.
- [32] J. Wan, J. Song, Z. Yang, D. Kirsch, C. Jia, R. Xu, J. Dai, M. Zhu, L. Xu, C. Chen, Y. Wang, Y. Wang, E. Hitz, S. D. Lacey, Y. Li, B. Yang, L. B. Hu, *Adv. Mater.*, 29 (2017) 1703331.
- [33] Y. Chen, X. Guo, J. Wang, W. He, V. V. Silberschmidt, S. Wang, Z. Tao, H. Xu, *J. Appl. Polym. Sci.*, 132 (2015) 41889.
- [34] J. Chen, X. Huang, Y. Zhu, P. Jiang, *Adv. Funct. Mater.*, 27 (2017) 1604754.
- [35] X. Huang, C. Zhi, P. Jiang, D. Golberg, Y. Bando, T. Tanaka, *Adv. Funct. Mater.*, 23 (2013) 1824-1831.
- [36] W. Jin, L. Yuan, G. Liang, A. Gu, *ACS Appl. Mater. Interfaces*, 6 (2014) 14931-14944.
- [37] E. Mu, Z. Wu, Z. Wu, X. Chen, Y. Liu, X. Fu, Z. Hu, *Nano energy*, 55 (2019) 494-500.
- [38] P. Min, J. Liu, X. Li, F. An, P. Liu, Y. Shen, N. Koratkar, Z. Yu, *Adv. Funct. Mater.*, 28 (2018) 1805365.
- [39] L. Zhang, R. Li, B. Tang, P. Wang, *Nanoscale*, 8 (2016) 14600-14607.

- [40] T. Ding, L. Zhu, X. Wang, K. Chan, X. Lu, Y. Cheng, G. Ho, *Adv. Energy Mater.*, 8 (2018) 1802397.

Journal Pre-proof



Journal Pre-proof



Journal Pre-proof

## Highlights

- The design of nacre-biomimetic membrane for high temperature thermal conductance.
- The membrane exhibits outstanding mechanical performances
- The membrane shows ultrahigh in-plane thermal conductivity and flame resistance.
- The membrane enables high temperature cooling of electronics.

Journal Pre-proof

**Jiemin Wang** has achieved his doctoral degree at Institute for Frontier Materials, Deakin University, Australia in Dec. 2019. He also has obtained his Master degree in Dec. 2012 with the major of Polymer Science and Engineering from The University of Manchester, UK and bachelor degree in June 2011 with the major of Polymer Materials Science and Engineering in Sichuan University, China. His current research interests focus on the nanocomposites and porous materials for environmental and energy applications.

**Dr Weiwei Lei** is a Senior Research Fellow at the Institute for Frontier Materials, Deakin University, Australia. He received his Ph.D. degree from Jilin University in 2009. From 2010 to 2011, he worked as a research fellow at Max Planck Institute of Colloids and Interfaces in Germany. Afterwards, he was awarded an Alfred Deakin Postdoctoral Research Fellowship (2011) and ARC Discovery Early Career Researcher (2014) at Deakin University. His research includes the synthesis of two- and three-dimensional nanomaterials and their applications in sustainable energy and water applications.

The authors declare no competing financial interest.

Journal Pre-proof